Inorg. Chem. **2009**, *48*, 2880−2886

A Theoretical Study of the Magnetic Circular Dichroism Spectrum for Sulfite Oxidase Based on Time-Dependent Density Functional Theory

Elizabeth Hernandez-Marin, Michael Seth, and Tom Ziegler*

Department of Chemistry, University of Calgary, Calgary, Alberta, Canada, T2N 1N4

Received October 1, 2008

We present a theoretical study of the temperature-dependent magnetic circular dichroism (MCD) spectrum for complexes modeling the molybdoenzyme sulfite-oxidase (**1**) in its Mo(V) oxidation state. The theoretical study was based on a newly implemented time-dependent density functional method that takes into account first-order perturbations due to spin−orbit coupling and a constant magnetic field. It was possible, on the basis of the theoretical calculations, to give a full assignment of the MCD spectrum for **1** and interpret the C term of each band in the experimental MCD spectrum in terms of spin−orbit couplings between specific excited states and between excited states and the ground state.

Introduction

Enzymes with a mononuclear molybdenum active center are known to contain at least one molybdopterin cofactor. This cofactor is coordinated to the molybdenum and consists of a pyran fused to a pterin ring (composed of a pyrazine ring and a pyrimidine ring). In addition, the pyran ring contains two thiolates, which bind to the metal (Figure 1). The majority of molybdoenzymes can be classified into three families represented by xanthine oxidase, sulfite oxidase (SO), and dimethylsulfoxide reductase.[1] Sulfite oxidase catalyzes the oxidation of sulfite to sulfate, the terminal reaction in the oxidative degradation of the sulfur-containing amino acids cysteine and methionine.[2] In this enzyme, molybdenum is coordinated by five ligands with an approximately square-pyramidal coordination geometry. The equatorial plane is occupied by three sulfur ligands and one water/hydroxo ligand, whereas an oxo group occupies the axial position.[3] According to the postulated mechanism for sulfite oxidase,[4] the oxidative half-cycle consists of two one-electron intramolecular transfers to obtain first Mo(V) and then Mo(VI). The spectroscopic studies on the active site of SO and related synthetic analogs represent an important step toward the understanding of the roles played by the ligands for the activity of the enzyme.

Among the spectroscopic methods, magnetic circular dichroism (MCD) is useful in the investigation of the electronic and geometric structure of transition metal complexes,[5] including those of biological importance.[6−8] It has further become possible in recent years to simulate MCD spectra from first principles by the implementation of computer codes based on time-dependent density functional theory (TDDFT)[9−12] or ab initio wave function methods[13−15] for both closed-[9−11,13,14] and open-shell[12,15] species.

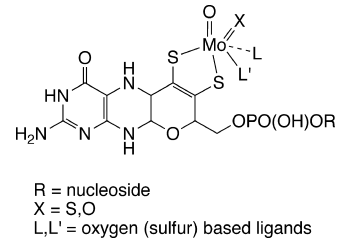

Figure 1. Molybdopterin cofactor.

* To whom correspondence should be addressed. E-mail: ziegler@ucalgary.ca.

(1) Basu, P.; Stolz, J.; Smith, M. *Curr. Sci.* **2003**, *84*, 1412.
(2) Hille, R. *Chem. Rev.* **1996**, *96*, 2757.
(3) Kisker, C.; Schindelin, H.; Pacheco, A.; Wehbi, W.; Garret, R.; Rajagopalan, K.; Enemark, J.; Rees, D. *Cell* **1997**, *91*, 973.
(4) Wilson, H.; Rajagopalan, K. *J. Biol. Chem.* **2004**, *279*, 15105.
(5) Mack, J.; Stillman, M.; Kobayashi, N. *Coord. Chem. Rev.* **2007**, *251*, 429.
(6) Decker, A.; Rohde, J.; Klinker, E.; Wond, S.; Que, L.; Solomon, E. *J. Am. Chem. Soc.* **2007**, *129*, 15983.
(7) Kennepohl, P.; Neese, F.; Schweitzer, D.; Jackson, H.; Kovacs, J.; Solomon, E. *Inorg. Chem.* **2005**, *44*, 1826.
(8) Mason, W. *A Practical Guide to Magnetic Circular Dichroism Spectroscopy*; John Wiley & Sons: New York, 2007.
(9) Krykunov, M.; Seth, M.; Ziegler, T.; Autschbach, J. *J. Chem. Phys.* **2007**, *127*, 244102.
(10) Seth, M.; Krykunov, M.; Ziegler, T.; Autschbach, J.; Banerjee, A. *J. Chem. Phys.* **2008**, *128*, 144105.
(11) Seth, M.; Krykunov, M.; Ziegler, T.; Autschbach, J. *J. Chem. Phys.* **2008**, *128*, 234102.
(12) Seth, M.; Ziegler, T.; Autschbach, J. *J. Chem. Phys.* **2005**, *122*, 094112.

10.1021/ic801875u CCC: $40.75
Published on Web 02/23/2009

MCD spectroscopy is based on the measurement of the difference in absorbance between left circularly polarized (lcp) light and right circularly polarized (rcp) light of a sample that is under the influence of a strong magnetic field oriented parallel to the direction of light propagation. The difference in absorbance is defined as $\Delta A = A_- - A_+$, where A_- and A_+ are lcp and rcp absorbance, respectively.[8]

Expressions have been developed to describe the MCD dispersion (characterized by A, B, and C terms according to the line shape) as a linear function of the applied magnetic field for a sample of randomly oriented molecules:[16]

$$\frac{\Delta A}{E} = \gamma B\left[A_1\left(-\frac{\partial f(E)}{\partial E}\right) + \left(B_o + \frac{C_o}{kT}\right)f(E)\right] \qquad (1)$$

where γ is a collection of constants, k is the Boltzmann constant, T is the temperature, B is the field strength of the applied magnetic field, $f(E)$ is a line shape function, and E is the energy of the incident radiation. A_1, B_o, and C_o are characteristic parameters that are specific to a given molecule and to the specific transition under study.

The A term is due to the Zeeman splitting of a degenerate ground or excited state. The B term is caused by the magnetic field inducing mixing of states, and the C term is due to a change in the population of molecules over the Zeeman sublevels of the ground state.

Paramagnetic sites that possess spin degeneracy show MCD due to spin−orbit coupling. The C terms observed for ground-state spin-degenerate molecules are usually much more intense than A or B terms at low temperatures; therefore, the C terms dominate the MCD spectrum in the spectroscopy of metalloenzymes with paramagnetic metal centers.[17]

In this study, we investigate the simulated MCD spectrum of a molybdenum model complex based on the active site of sulfite oxidase. The objective is to identify the transitions that give rise to the MCD signal and detail the origin of the C terms involved in the spectrum.

Computational Methods and Details

Let us consider a situation where the degeneracy of a ground state is broken due to the presence of a magnetic field. With the splitting of the Zeeman sublevels, the level with the lowest energy will become preferably Boltzmann-populated. Under those conditions, there will be a difference in the intensity of the absorbance of lcp and rcp light, as depicted in Figure 2. At very low temperatures and high magnetic fields, only the lowest level will be populated, and the signal reaches its maximum (saturation).[18]

The type of C term described above is typical for systems with a spatially degenerate ground state, and it requires only a magnetic perturbation.[19] A system with a spin-degenerate ground state does not exhibit temperature-dependent C terms by the mechanism

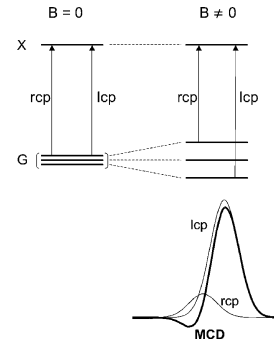

Figure 2. Energy levels for the transition between ground state (G) and excited state (X). This mechanism requires the ground state to be magnetically degenerate for the existence of C terms.

described above, although the ground-state levels are split by a magnetic field. However, temperature-dependent C terms are possible for systems with a spin-degenerate ground state if, in addition to the magnetic perturbation, one allows for the coupling between states due to spin−orbit coupling.[20,21] We shall in the current study concentrate exclusively on the calculation of this type of C parameter.

We have, as an extension to previous MCD schemes,[10,11] implemented a method that calculates the temperature-dependent C_o for a spin-degenerate ground state by including spin−orbit perturbations.[22] This implementation into the ADF program makes use of TDDFT to describe electronic excitations[23] and the zero-order regular approximation formalism to include relativistic effects.[24]

The C parameter induced by the perturbation of the transition dipole J in the γ direction by spin−orbit coupling can be defined as[22]

$$C_J = -\frac{4i}{3|G|}\sum_M M^2 \sum_{\alpha\beta\gamma} \varepsilon_{\alpha\beta\gamma}\langle A|M^\alpha|J\rangle^{(1)\gamma}\langle J|M^\beta|A\rangle^{(0)} \qquad (2)$$

where $i = \sqrt{-1}$, $|G|$ is the degeneracy of the ground state, M is the spin quantum number, $\varepsilon_{\alpha\beta\gamma}$ is the Levi−Civita symbol, M^α and M^β correspond to Cartesian components of the electric dipole moment operator, A refers to the ground state, J refers to a given excited state, and the superscripts (1) and (0) indicate the first-order perturbed and unperturbed integrals, respectively.

The perturbed integral $\langle A|M^\alpha|J\rangle^{(1)\gamma}$ can be written as

$$\langle A|M^\alpha|J\rangle^{(1)\gamma} = \langle A^{(1)\gamma}|M^\alpha|J^{(0)}\rangle + \langle A^{(0)}|M^\alpha|J^{(1)\gamma}\rangle \qquad (3)$$

The first term on the right-hand side of eq 3 corresponds to the perturbation of the ground state A by spin−orbit coupling and the second to perturbation of the excited state J. These perturbations are often described in terms of mixing of other states with the ground or excited state, respectively. Such a description leads to a sum-over-states (SOS) expression:

(13) Ganyushin, D.; Neese, F. *J. Chem. Phys.* **2008**, *128*, 114117.
(14) Solheim, H.; Ruud, K.; Coriani, S.; Norman, P. *J. Chem. Phys.* **2008**, *128*, 094103.
(15) Bolvin, H. *Inorg. Chem.* **2007**, *46*, 417.
(16) Stephens, P. *Annu. Rev. Phys. Chem.* **1974**, *25*, 201.
(17) Kirk, M.; Peariso, K. *Curr. Opin. Chem. Biol.* **2003**, *7*, 220.
(18) Lehnert, N.; DeBeer George, S.; Solomon, E. *Curr. Opin. Chem. Biol.* **2001**, *5*, 176.
(19) Stephens, P. *J. Chem. Phys.* **1965**, *43*, 4444.
(20) Denning, R.; Spencer, J. *Symp. Faraday Soc.* **1969**, *3*, 84.
(21) Denning, R. *J. Chem. Phys.* **1966**, *45*, 1307.
(22) Seth, M.; Ziegler, T.; Autschbach, J. *J. Chem. Phys.* **2008**, *129*, 104105.
(23) Casida, M. In *Advances in Density Functional Methods*; Chong, D. P., Ed.; World Scientific: Singapore, 1995; Vol. 1, p 155.
(24) van Lenthe, E.; Baerends, J.; Snijders, J. *J. Chem. Phys.* **1993**, *99*, 4597.

$$\langle A|M^{\alpha}|J\rangle^{(1)\gamma} = \sum_{K' \neq A} \langle K'^{(0)}|M^{\alpha}|J^{(0)}\rangle \frac{\langle K'^{(0)}|H_{SO}^{\gamma}|A^{(0)}\rangle}{E_{K'} - E_A} + \sum_{K \neq J} \langle A^{(0)}|M^{\alpha}|K^{(0)}\rangle \frac{\langle J^{(0)}|H_{SO}^{\gamma}|K^{(0)}\rangle}{E_K - E_J} \quad (4)$$

where H_{SO} is the spin−orbit operator. Equation 4 is written in the SOS form for the sake of qualitative interpretation of our results. In the actual evaluation of C, use is made of response theory.[22] For qualitative analysis purposes, inspection of eqs 2 and 4 allows one to write a simplified expression for the C term as

$$C_J = C_J^{G} + C_J^{E} \quad (5)$$

Here, C_J^{G} comes from the first term on the right-hand side of eq 4, representing the coupling between the ground state (A) and excited states (K') due to spin−orbit coupling. Likewise, C_J^{E} is the contribution to the C term from the perturbation of the excited state J by other excited states K due to spin−orbit coupling, as expressed by the second term on the right side of eq 4. These contributions are graphically depicted in Figure 3. It has been anticipated from previous studies that the contributions due to spin−orbit coupling of states J and K (C_J^{E}) dominate the total value of the C term,[25] whereas a smaller but not negligible contribution is likely to arise from terms involving spin−orbit coupling of state K' and the ground state (C_J^{G}).[25] A third contribution, usually considered to be negligible, to the C term arises from the spin−orbit coupling of the ground state with low-lying excited states. However, recently, it has been discussed that at least in the case of low-spin iron(III) porphyrins the coupling between the ground state and low-lying excited states should actually be considered.[26] Because in the current study we are dealing with d^1 systems, we do not a priori expect an important contribution from the third mechanism. We shall in the following analyze the relative contributions of C_J^{G} and C_J^{E} to the C term. A detailed account of how C_J^{G} and C_J^{E} are calculated within TDDFT can be found elsewhere.[22]

The calculations were performed with the modified version[22] of the ADF[27] program using the Becke−Perdew exchange correlation functional (BP86)[28−30] and a standard triple-ζ STO basis with one set of polarization functions for all atoms. The frozen core approximation was used. The core was defined as $1s^2$ for carbon, nitrogen, and oxygen; $1s^22s^22p^6$ for sulfur; and $1s^22s^22p^63s^23p^64s^23d^{10}$ for molybdenum. All calculations were spin-unrestricted.

The molybdenum complex $[MoO(SCH_3)(dith)OH]^{-1}$ (dith = $^{-}SCH_2CH_2S^{-}$) used for the calculation of the C parameters is shown in Figure 4. The optimized geometry had as the starting point a structure constructed from the Cartesian coordinates provided by the chicken sulfite oxidase (CSO) X-ray structure.[3] In order to have a model complex of a size reasonable for the computational study, the cysteine 185 was substituted with methyl thiolate and the molybdopterin cofactor with ene-1,2-dithiolate. The use of ene-1,2-dithiolate seems to be a reasonable choice since it contains the thiolate and ethylene groups that constitute a ring, such as in Figure 1. Previous computational studies on molybdoenzymes have also made use of a smaller ligand to model the molybdopterin cofactor.[31] A much larger model containing the whole molybdopterin cofactor was additionally constructed. A geometry optimization and subsequent simulation of the absorption spectrum for this larger complex were performed. The results from such calculations are summarized in the Supporting Information. They indicate that the use of the whole molybdopterin cofactor is not necessary to obtain some insight into the MCD spectrum of the enzyme.

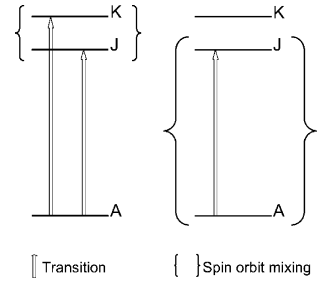

Figure 3. Origin of the contributions to the C term due to the spin−orbit mixing. Left: C_J^{E}, due to perturbation of excited state J. Right: C_J^{G}, due to perturbation of ground state A.

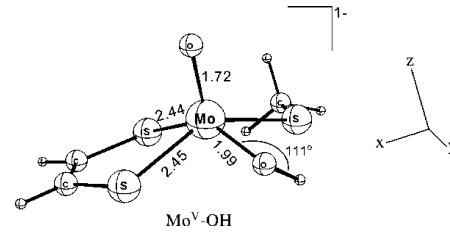

Mo^{V}-OH

Figure 4. Model used for the calculation of MCD C terms.

Finally, for the simulation of the MCD spectrum, the band-shape functions f (eq 1) of choice were normalized Gaussian functions:

$$f_J(E) = \frac{1}{\sqrt{\pi} W_J} e^{-\left(\frac{E_J - E}{W_J}\right)} \quad (6)$$

and their derivatives centered around the calculated excitation energy E_J. The bandwidth parameters were chosen to approximately reproduce the experimental spectrum.

Results and Discussion

The MCD spectrum of the [Mo(V):Fe(II)] state of the CSO enzyme has been measured.[32] The use of temperature-difference MCD techniques revealed C terms arising from the Mo(V) site. Due to interference from the ferrous center, it was not possible to observe MCD signals in some regions of the spectrum (17 000−20 000 and 23 000−24 000 cm^{-1}). The experimental spectrum is shown in Figure 5. This spectrum consists of two positive C terms at 22 250 (C_1) and 26 500 cm^{-1} (C_2) and one negative C term at 31 000 cm^{-1} (C_3). The assignment of the bands was based on the results obtained from spectroscopic and computational studies on biomimetic oxomolybdenum complexes.[33] The 22 250 cm^{-1} (C_1) transition was assigned to a weak $S_{cys}^{\sigma} \rightarrow$ Mo d_{xy} charge-transfer excitation (S_{cys}^{σ} corresponds to a σ-bonding

(25) Neese, F.; Solomon, E. *Inorg. Chem.* **1999**, *38*, 1847.
(26) Paulat, F.; Lehnert, N. *Inorg. Chem.* **2008**, *47*, 4963.
(27) Te Velde, G.; Bickelhaupt, F.; Baerends, E.; van Gisbergen, S.; Guerra, C.; Snijders, J.; Ziegler, T. *J. Comput. Chem.* **2001**, *22*, 931.
(28) Becke, A. *Phys. Rev. A: At., Mol., Opt. Phys.* **1998**, *38*, 3098.
(29) Perdew, J. *Phys. Rev. B: Condens. Matter Mater. Phys.* **1986**, *33*, 8822.
(30) Perdew, J. *Phys. Rev. B: Condens. Matter Mater. Phys.* **1986**, *34*, 7406.
(31) (a) Zhang, X. H.; Wu, Y. D. *Inorg. Chem.* **2005**, *44*, 1466. (b) Amano, T.; Ochi, N.; Sato, H.; Sakaki, S. *J. Am. Chem. Soc.* **2007**, *129*, 8131.
(32) Helton, M.; Pacheco, A.; McMaster, J.; Enemark, J.; Kirk, M. *J. Inorg. Biochem.* **2000**, *80*, 227.
(33) McNaughton, R.; Tipton, A.; Rubie, N.; Conry, M.; Kirk, M. *Inorg. Chem.* **2000**, *39*, 5697.

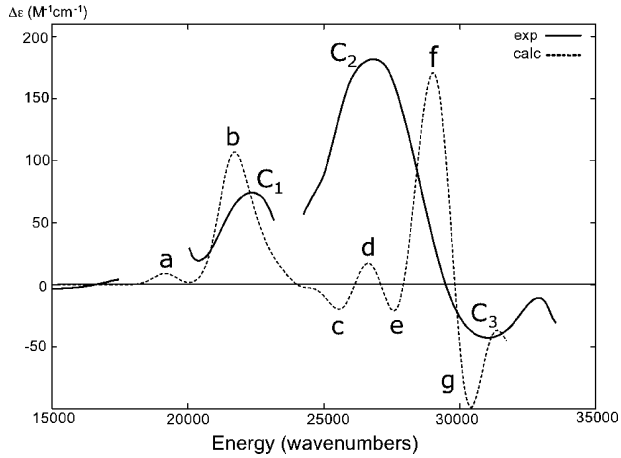

Figure 5. Experimental (solid line) and simulated (broken line) MCD spectra. Experimental bands are C_1, C_2, and C_3. The calculated bands are marked with letters a−g.

cysteine thiolate sulfur orbital). The C term at 26 500 cm^{-1} (C_2) was hypothesized to originate from a $S^{op}_{dith} \rightarrow$ Mo $d_{xz,yz}$ transition where S^{op}_{dith} is an out-of-plane dithiolate sulfur orbital (the plane was defined as the equatorial plane orthogonal to the Mo═O bond). The 31 000 cm^{-1} (C_3) transition was not assigned. Additionally, considering the results obtained with the synthetic analogs,[32] a C-term feature was anticipated at ≈19 000 cm^{-1} due to a $S^{ip}_{dith} \rightarrow$ Mo d_{xy} charge-transfer transition, where S^{ip}_{dith} is an in-plane sulfur-based dithiolate orbital.[32] However, the interference of the ferrous center in this region prevents the observation of any signal between 17 000 and 20 000 cm^{-1} for the real system.

The simulated MCD spectrum exhibits four positive MCD bands with maximum intensities at 19 211, 21 711, 26 645, and 29 079 cm^{-1} (a, b, d, and f in Figure 5) and three negative MCD bands at 25 568, 27 500, and 30 395 cm^{-1} (c, e, and g in Figure 5). The agreement between the experimental and simulated MCD spectra is reasonably good. In particular, a broadening of the band-shape functions ($f(E)$) for c, d, e, and f of the simulated spectrum might cause those MCD bands to appear as one. We suggest that the observed broad MCD band C_2 of Figure 5 consists of c, d, e, and f from the simulated spectrum.

We shall now turn to the assignment and interpretation of the MCD spectra shown in Figure 5. To this end, we start by discussing the nature of each calculated transition $A \rightarrow J$ in terms of contributions from one-electron excitations. Later we describe the origin of each C_o in terms of contributions from the mixing of the excited state J with other excited states (K) as well as the coupling of the ground state (A) with excited states (J, K').

The simulated absorption spectrum is shown in Figure 6. It consists of four bands with maxima at 19 383 (B_1), 21 906 (B_2), 24 957 (B_3), and 29 150 (B_4) cm^{-1}. The B_1 band consists of transitions 1 and 2, while the B_2 band contains transitions 3 and 4. Likewise, the band B_3 comprises transitions 5−7, and B_4 includes transitions 9−15. The composition of the mentioned excitations is listed in Table 1. Additionally, the key orbitals involved in the one-electron excitations are presented in Figures 7 and 8.

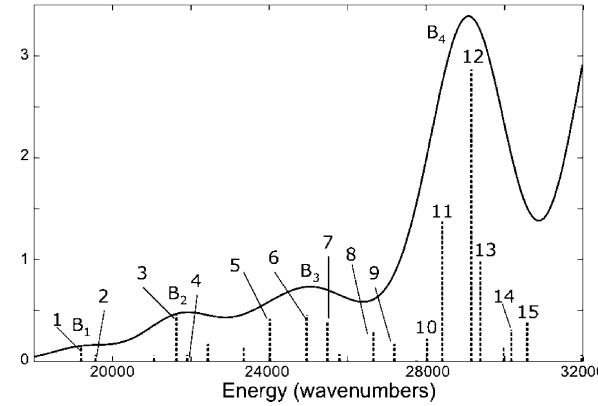

Figure 6. Simulated absorption spectrum for the model Mo^V−OH. Four bands, B_1 to B_4, are marked. The bars underneath the spectrum line indicate the absorbance of each transition contributing to the band.

Table 1. Calculated Excitation Energies, Oscillator Strength (f), and Assignment of Selected One-Electron Excitations for Model Complex Mo^V−OH

band	label	excitation energy	composition[b]	%	f
B_1	1	19200	β S_{dith} $p_{z'} \rightarrow$ Mo d_{xy}	98.9	0.0010
	2	19560	α Mo $d_{xy} \rightarrow$ Mo d_{xz}	93.9	0.0004
B_2	3	21630	β S_{Cys} $p_x \rightarrow$ Mo d_{xy}	90.6	0.0029
	4	21910	α Mo $d_{xy} \rightarrow$Mo d_{yz}	80.6	0.0004
B_3	5	24010	β S_{dith} $p_y \rightarrow$ Mo d_{xy}	77.1	0.0026
	6	24950	α Mo d_{xy}-S_{dith} $p_z \rightarrow$ Mo d_{yz}	80.4	0.0029
			β S_{dith} $p_z \rightarrow$ Mo d_{yz}	13.0	
	7	25480	α S_{Cys}[c] $p_z \rightarrow$ Mo d_{xz}	77.5	0.0025
			β S_{Cys} $p_z \rightarrow$ Mo d_{xz}	17.6	
	8	26660	β O_{OH} $p_{z,y} \rightarrow$ Mo d_{xy}	93.7	0.0018
	9	27090	α Mo d_{xy}-S_{dith} $p_z \rightarrow$ Mo $d_{x^2-y^2}$	37.8	0.0011
			β S_{dith} $p_z \rightarrow$ Mo $d_{x^2-y^2}$	17.1	
B_4	10	28020	α S_{Cys} $p_z \rightarrow$ Mo d_{yz}	80.5	0.0013
	11	28410	β S_{Cys} $p_z \rightarrow$ Mo d_{xz}	61.6	0.0085
	12	29150	α Mo d_{xy}-S_{dith} $p_z \rightarrow$ Mo $d_{x^2-y^2}$	31.9	0.0180
			β S_{dith} $p_z \rightarrow$ Mo $d_{x^2-y^2}$	25.7	
	13	29390	α Mo $d_{xy} \rightarrow$ Mo d_{z^2}	43.9	0.0062
			β S_{dith} $p_z \rightarrow$ Mo $d_{x^2-y^2}$	14.3	
			β S_{dith} $p_z \rightarrow$ Mo d_{z^2}	13.0	
	14	30170	β S_{Cys} $p_z \rightarrow$ Mo d_{yz}	73.3	0.0019
	15	30580	α Mo d_{xy}-S_{dith} $p_z \rightarrow$ Mo $d_{x^2-y^2}$	62.7	0.0025
			α Mo $d_{xy} \rightarrow$ Mo d_{z^2}	11.5	

[a] Energies in cm^{-1}. [b] The orbitals are shown in Figures 7 and 8. [c] The label "Cys" corresponds to the methyl thiolate ligand in the model complex.

The weak excitation at 19 200 cm^{-1} (1) can be considered as a ligand-to-metal transition, where the electron is excited from a molecular orbital mainly formed by the out-of-plane sulfur dithiolate p_z orbitals to a Mo d_{xy} orbital. A d−d transition occurs at 19 560 cm^{-1} (2) between the semioccupied molecular orbital (SOMO) d_{xy} and d_{xz} molybdenum levels. A simplified diagram with the highest occupied and lowest unoccupied orbital levels is shown in Figure 9. For the next excitation at 21 630 cm^{-1} (3), the major contribution is from the transition between the p_x methyl thiolate sulfur[34] and the metal d_{xy} orbitals. Another weak d−d excitation between the SOMO d_{xy} and d_{yz} molybdenum orbitals occurs at 21 910 cm^{-1} (4). On one hand, excitations 5, 6, 9, and 12 are ligand-to-metal transitions where dithiolate is the relevant ligand. Excitation 5 (24 010 cm^{-1}) involves the transition

(34) To keep some connection of our model with the molybdoenzyme, we use the subscript "Cys" when referring to the methyl thiolate ligand.

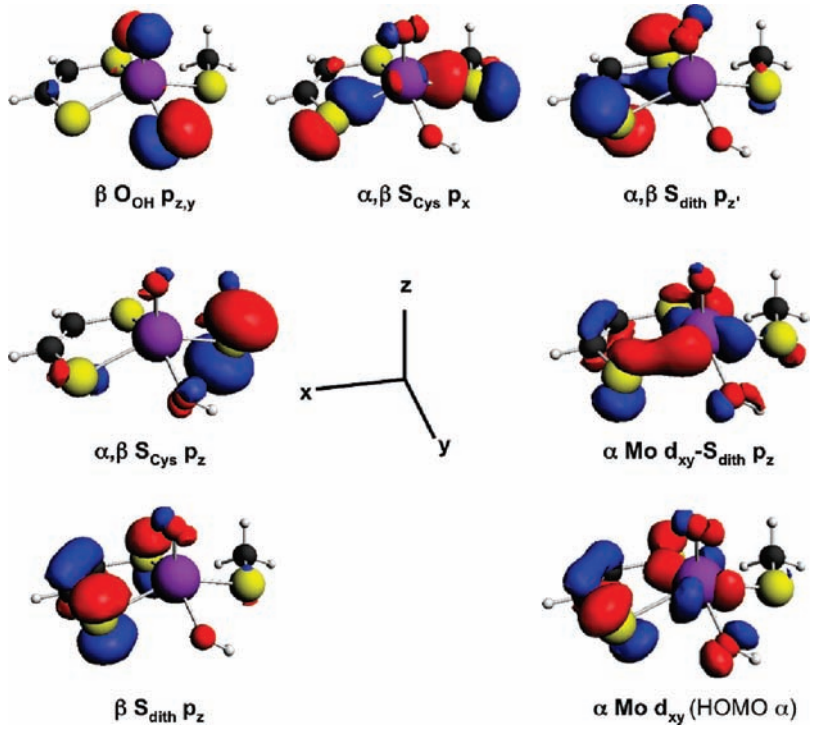

Figure 7. Key occupied orbitals for the model complex $Mo^{V}-OH$.

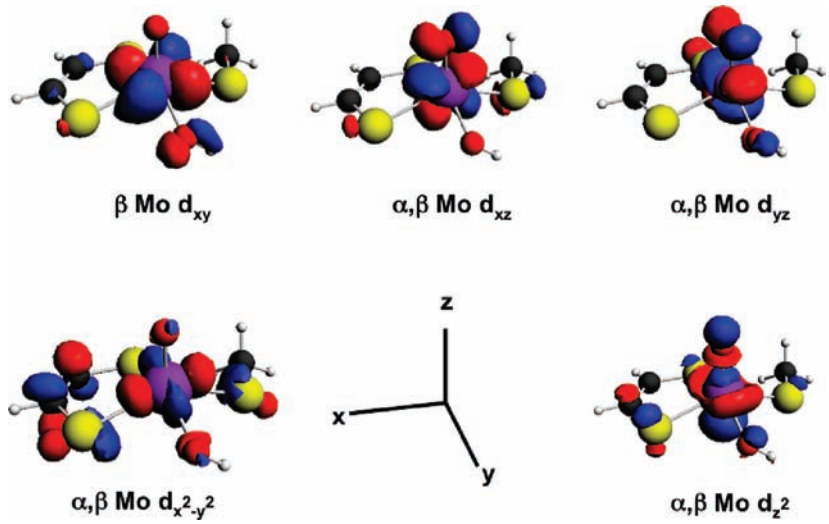

Figure 8. Key virtual orbitals for the model complex $Mo^{V}-OH$.

from the sulfur p_y orbital to the molybdenum d_{xy} orbital. Excitation 6 (24 950 cm^{-1}) consists of the transition from sulfur p_z to molybdenum d_{yz}. The two excitations 9 (27 090 cm^{-1}) and 12 (29 150 cm^{-1}) consist of the transition from sulfur p_z to molybdenum $d_{x^2-y^2}$. On the other hand, the ligand-to-metal transitions involving the methyl thiolate ligand (Cys) occur at 25 480 (7), 28 020 (10), 28 410 (11), and 30 170 cm^{-1} (14) with transitions from the sulfur p_z orbital to the molybdenum d_{yz} in the case of excitations 10 and 14, and to d_{xz} for excitations 7 and 11. There is one transition (8) with participation from the hydroxide ligand at 26 655 cm^{-1}. Excitation 13 at 29 390 cm^{-1} includes a d−d transition between the d_{xy} and d_{yz} molybdenum orbitals and, to a lesser extent, ligand-to-metal transitions between the dithiolate sulfur p_z and the Mo $d_{x^2-y^2}$ and d_{z^2} orbitals. The most intense absorption corresponds, as mentioned earlier, to the transition between the sulfur p_z dithiolate ligand and the Mo $d_{x^2-y^2}$ orbitals at 29 150 cm^{-1}. This transition was assigned to be between the p_z dithiolate sulfur and the Mo $d_{xz,yz}$ orbital pair on the basis of calculations involving model systems of C_{4v} or C_s symmetry.[35,36] However, those models did not include a thiolate ligand or an equatorial hydroxyl ligand. We will expand on this discrepancy later in connection with the discussion of the calculated MCD spectrum.

Turning back to the interpretation of the MCD data, Figure 10 shows the simulated normalized MCD spectrum along with the individual calculated parameters. Table 2 contains

(35) Carducci, M. D.; Brown, C.; Solomon, E. I.; Enemark, J. H. *J. Am. Chem. Soc.* **1994**, *116*, 11856.
(36) Inscore, F. E.; McNaughton, R.; Westcott, B. L.; Helton, M. E.; Jones, R.; Dhawan, I. K.; Enemark, J. H.; Kirk, M. *Inorg. Chem.* **1999**, *38*, 1401.

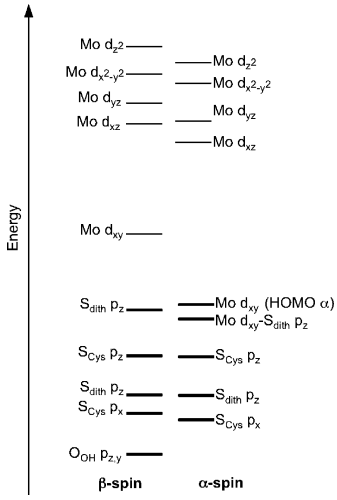

Figure 9. Molecular orbital energy level diagram for α and β spins from model Mo^{V}−OH.

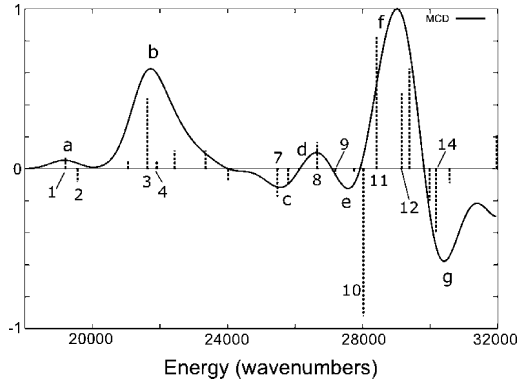

Figure 10. Normalized simulated MCD spectrum of the model complex Mo^{V}−OH. The bars indicate the relative intensity of the calculated C term for each excitation.

Table 2. Calculated C-Term Parameters[a] for Model Complex Mo^{V}−OH

C term	J^b	C_J	C_J^G	$C_{JK'}^G$	K'	C_J^E	C_{JK}^E	K
a	1	8.72[c]	6.22[d]	5.24[e]	1	2.50[f]	1.46[g]	3
	2	−5.65	−1.41			−4.24	−1.17	12
b	3	33.10	37.92	28.69	3	−4.82	−5.91	4
c	7	−12.25	0.92			−13.17	−4.55	10
							−2.15	14
d	8	10.85	0.10			10.75	2.44	9
							1.15	12
e	10	−73.56	−5.15			−68.41	−31.83	11
							−5.80	12
f	11	57.25	−2.79			60.04	31.70	10
	12	41.73	1.97			39.76	14.96	11
							13.88	14
g	14	−31.30	6.06			−37.36	−14.22	12
							−11.86	11

[a] Values in au $\times 10^{-4}$. For details, see eqs 2−5. [b] See Table 1 for details on the excitations. [c] C_J is the C parameter for excitation J. [d] C_J^G is the contribution to C_J due to the spin−orbit coupling perturbation of the ground state. [e] $C_{JK'}^G$ is the individual major contribution to C_J^G, due to the mixing of the ground state with excitation K'. [f] C_J^E is the contribution to C_J from the perturbation of the excited state J. [g] C_{JK}^E is the contribution to C_J^E from the mixing of excited states J and K.

the relevant calculated C_J parameters and its contributions from the spin−orbit coupling perturbation of the ground state and the excited state (C_J^G and C_J^E, respectively). Table 2 includes the largest individual contributions (C_{JK}^E) to the total value of C_J^E due to interaction of excited states J and K as well as the major sources ($C_{JK'}^G$) to C_J^G from the coupling between excited states K' and the ground state A. They generally fall in the range of 10−60% of the total value. The rest of the individual contributions are around 1% and were deemed not relevant for qualitative analysis purposes.

Now, we shall elaborate on the origin of the simulated C terms labeled from a to f in Figure 10. Two excitations around 19 000 cm^{-1} give rise to the positive MCD band "a" (Figure 10). A positive C parameter is calculated at 19 200 cm^{-1} (excitation 1). We assigned it to an $S_{dith} \rightarrow$ Mo d_{xy} transition, in agreement with Kirk et al.[32] In this case, the perturbation of the ground state by mixing with excitation 1 is the dominant term. The adjacent negative C parameter is from a Mo $d_{xy} \rightarrow d_{xz}$ transition (excitation 2, Table 1), and it arises from the spin−orbit coupling interaction between excited states 2 and 12 (dithiolate-to-metal transition).

Next, the experimental C term at 22 250 cm^{-1} (C_1, Figure 5) corresponds to band "b" of the calculated spectrum. This band is mostly due to the C parameter calculated at 21 630 cm^{-1} (excitation 3), as shown in Figure 10. It is accordingly assigned to the S_{Cys} $p_x \rightarrow$ Mo d_{xy} transition (or a $S_{cys}^{\sigma} \rightarrow$ Mo d_{xy} transition following Kirk et al. nomenclature). This parameter is dominated by the perturbation of the ground state through interactions with excitation 3. The smaller C_J^E contribution is mostly due to the interaction with excitation 4 assigned as a Mo $d_{xy} \rightarrow d_{yz}$ transition.

As we already mentioned, the broad experimental signal C_2 at 26 500 cm^{-1} might contain signals "c", "d", "e", and "f" of the simulated spectrum (Figure 5). The weak negative band "c" is mainly attributed to the perturbation of the corresponding excitation 7 by mixing with excitations 10 and 14. These excitations are transitions from the S_{Cys} p_z orbital to the Mo d_{xz} (exc. 7) and Mo d_{yz} (exc. 10 and 14) orbitals, respectively. The positive, weak MCD band "d" comes from excitation 8 (hydroxide-to-metal). Table 2 shows that the term C_J^E accounts for 99% of the total C value. Here, excitation 8 (hydroxide-to-metal) mixes with 9 (dithiolate-to-Mo $d_{x^2-y^2}$ transition) and with excitation 12 as well. It should be noted that both excitations 9 and 12 involve the same orbitals. The other weak, negative band "e" seems to appear mostly due to the fact that the intense negative C parameter (−0.007356 au) from excitation 10 is adjacent to the positive and slightly less intense parameter (0.005725 au) at 28 413 cm^{-1} (excitation 11). The two excitations are mainly C_J^E in nature and arise from the mutual interaction of both excited states. However, additional mixing between excitations 10 and 12 gives rise to the difference in the total values. The nature of those transitions is S_{Cys} $p_z \rightarrow$ Mo d_{yz} and S_{Cys} $p_z \rightarrow$ Mo d_{xz}, respectively. Figure 10 shows that those two excitations might constitute a pseudo-A term. The experimental MCD spectrum of LMoObdt (L = hydrotris(3-5-dimethyl-1-pyrazolyl)borate; bdt = 1,2-benzenedithiolate) contained a signal with a pseudo-A-term character and was assigned to excitations of the type S_{dith} $p_z \rightarrow$ Mo $d_{xz,yz}$ (the d_{xz} and d_{yz} orbitals were nearly degenerate).[35] However, the LMoObdt molecule does not have a thiolate ligand, in contrast to our model complex. Thus, our calculations indicate the effective influence of the equatorial thiolate

ligand on the electronic structure of the enzyme. Last, the dominant signal with label "f" is mostly due to the dithiolate-to-metal transition at 29 150 cm^{-1} (excitation 12), as suggested by Kirk et al.[32] The origin of this C parameter is due to the mixing of the excited state with excitations 11 and 14, both thiolate-to-metal transitions.

Experimentally, the MCD spectra of the high- and low-pH forms are indistinguishable.[32] Our calculations show only one transition involving the hydroxide ligand giving rise to a weak negative C term. One structural difference between the high- and low-pH species might be the orientation of the hydroxide;[37] thus, it is reasonable to expect the electronic transition to be similar in both cases.

Kirk et al. did not assign the signal at 31 000 cm^{-1} (C_3, Figure 5). Our calculations show that it arises from a transition, mainly $S_{Cys}\ p_z \rightarrow Mo\ d_{yz}$ (excitation 14). Table 2 indicates that its origin is mainly due to the interaction of the excited state with excitations 12 and 11, the latter described as a $S_{Cys} \rightarrow Mo\ d_{xz}$ transition.

Conclusions

We have presented a simulation of the MCD spectrum for a paramagnetic d^1 system, $[MoO(SCH_3)(dith)OH]^{-1}$. This molecule was constructed from an X-ray structure of the molybdoenzyme sulfite oxidase. The MCD simulation was based on a recent implementation that includes spin−orbit coupling. This new approach allows for the calculation of the temperature-dependent C terms of systems with spin-degenerate ground states.

Good agreement with the experimental spectrum from the enzyme was obtained. In line with the assignment made by Kirk et al.,[31] we found that the C term at 22 250 cm^{-1} arises from a $S_{Cys}\ p_x \rightarrow Mo\ d_{xy}$ transition. On the basis of data from inorganic compounds lacking a thiolate ligand,[35,36] Kirk et al. assigned the experimental C term at 26 500 cm^{-1} to a $S_{dith}\ p_z \rightarrow Mo\ d_{xz,yz}$ transition. Our results indicate that such a broad signal contains several excitations due to the following transitions: $S_{Cys}\ p_z \rightarrow Mo\ d_{yz}$, $S_{Cys}\ p_z \rightarrow Mo\ d_{xz}$, and $S_{dith}\ p_z \rightarrow Mo\ d_{x^2-y^2}$. Those findings seem to imply that the coordinated cysteine has an influence on the electronic spectrum of CSO. Furthermore, it is proposed that the experimental C term at 31 000 cm^{-1}, which was not previously assigned, corresponds to a $S_{Cys}\ p_z \rightarrow Mo\ d_{yz}$ transition. The simulation suggests that the regions between 17 000−20 000 and 23 000−24 000 cm^{-1} that were experimentally obscured by the presence of iron in the enzyme might contain both ligand-to-metal and d−d transitions in the first region and ligand-to-metal transitions in the second. The only time when the hydroxyl ligand participates in the excitation is in the 23 000−24 000 cm^{-1} region; the rest of the excitations involve the sulfur atoms of the dithiolate ligand or the sulfur atoms of the thiolate ligand (representing the cysteine coordinated to the molybdenum).

Acknowledgment. This work was supported by NSERC. T.Z. would like to thank the Canadian government for a Canada Research Chair.

Supporting Information Available: Results from geometry optimization and subsequent simulation of the absorption spectrum for a model containing the full molybdopterin cofactor are summarized. This material is available free of charge via the Internet at http://pubs.acs.org.

IC801875U

(37) Doonan, C. J.; Wilson, H. L.; Bennet, B.; Prince, R. C.; Rajagopalan, K. V.; George, G. N. *Inorg. Chem.* **2008**, *47*, 2033.